Antonie van Leeuwenhoek (2020) 113:1751–1766
https://doi.org/10.1007/s10482-019-01367-4

ORIGINAL PAPER

Alienimonas californiensis gen. nov. sp. nov., a novel Planctomycete isolated from the kelp forest in Monterey Bay

Alje S. Boersma · Nicolai Kallscheuer · Sandra Wiegand · Patrick Rast · Stijn H. Peeters · Rob J. Mesman · Anja Heuer · Christian Boedeker · Mike S. M. Jetten · Manfred Rohde · Mareike Jogler · Christian Jogler

Received: 23 June 2019 / Accepted: 26 November 2019 / Published online: 4 December 2019

Abstract Planctomycetes are environmentally and biotechnologically important bacteria and are often found in association with nutrient-rich (marine) surfaces. To allow a more comprehensive understanding of planctomycetal lifestyle and physiology we aimed at expanding the collection of axenic cultures with new isolates. Here, we describe the isolation and genomic and physiological characterisation of strain CA12^T obtained from giant bladder kelp (*Macrocystis pyrifera*) in Monterey Bay, California, USA. 16S rRNA gene sequence and whole genome-based phylogenetic analysis showed that strain CA12^T clusters within the family *Planctomycetaceae* and that it has a high 16S rRNA sequence similarity (82.3%) to *Planctomicrobium piriforme* DSM 26348^T. The genome of strain CA12^T has a length of 5,475,215 bp and a G+C content of 70.1%. The highest growth rates were observed at 27 °C and pH 7.5. Using different microscopic methods, we could show that CA12^T is able to divide by consecutive polar budding, without completing a characteristic planctomycetal lifestyle switch. Based on our data, we suggest that the isolated strain represents a novel species within a novel genus. We thus propose the name *Alienimonas* gen. nov. with *Alienimonas californiensis* sp. nov. as type species of the novel genus and CA12^T as type strain of the novel species.

Keywords Cell division · Marine bacteria · Planctomycetes · Primary metabolism · Carbohydrate active enzymes

Electronic supplementary material The online version of this article (https://doi.org/10.1007/s10482-019-01367-4) contains supplementary material, which is available to authorized users.

A. S. Boersma · N. Kallscheuer · S. Wiegand · S. H. Peeters · R. J. Mesman · M. S. M. Jetten · M. Jogler · C. Jogler (✉)
Department of Microbiology, Radboud University Nijmegen, Nijmegen, The Netherlands
e-mail: christian@jogler.de

P. Rast · A. Heuer · C. Boedeker · M. Jogler
Leibniz Institute DSMZ Braunschweig, Brunswick, Germany

M. Rohde
Central Facility for Microscopy, Helmholtz Centre for Infection Research, Brunswick, Germany

Introduction

Planctomycetes are environmentally important bacteria that are found across all aquatic habitats, where they act as key players in global carbon and nitrogen cycles (Wiegand et al. 2018). Together with members of the phyla Verrucomicrobia, Chlamydiae and others, Planctomycetes belong to the medically and biotechnologically relevant PVC superphylum (Wagner and Horn 2006). The phylum Planctomycetes itself is divided into two classes: Planctomycetia and

Phycisphaerae. The order *Planctomycetales* is the only validly named order within the Planctomycetia and consists of three families: *Planctomycetaceae*, *Isosphaeraceae* and *Gemmataceae*, with the vast majority of described planctomycetal species belonging to the family *Planctomycetaceae* (Scheuner et al. 2014; Kulichevskaya et al. 2016, 2017). The class *Phycisphaerae* consists of the orders *Phycisphaerales*, *Sedimentisphaerales* and *Tepidisphaerales*, which each consist of only one family (Fukunaga et al. 2009; Kovaleva et al. 2015; Spring et al. 2018). Anammox Planctomycetes make up the *Candidatus* Brocadiaceae clade, which holds this placeholder status due to the lack of axenic cultures (Peeters and van Niftrik 2019).

In the past, Planctomycetes were proposed to possess several eukaryotic traits, such as the lack of a peptidoglycan (PG) cell wall (König et al. 1984), a compartmentalised cell plan (Lindsay et al. 1997), a nucleus-like structure (Fuerst and Webb 1991) and the endocytosis-like uptake of macromolecules (Lonhienne et al. 2010). Thus, Planctomycetes were thought to bridge the gap between bacteria and eukaryotes (Lonhienne et al. 2010; Fuerst and Sagulenko 2011; Devos et al. 2013). However, with the development of novel microscopic techniques and genetic tools for Planctomycetes (Jogler et al. 2011; Rivas-Marin et al. 2016; Boedeker et al. 2017), these traits were recently refuted. Planctomycetes were found to have a PG cell wall (Jeske et al. 2015; van Teeseling et al. 2015). This observation, together with the finding that their closest relatives, the Verrucomicrobia, also contain PG (Rast et al. 2017), now suggests that all known free-living bacteria have a PG cell wall (Rast et al. 2017). With the exception of anammox Planctomycetes (Jogler 2014, Neumann et al. 2014), the proposed cell compartments were found to rather be exceptionally large invaginations of the cytoplasmic membrane (Santarella-Mellwig et al. 2013; Acehan et al. 2014; Boedeker et al. 2017). Consequentially, the cell plan of Planctomycetes was reinterpreted to more closely resemble that of Gram-negative bacteria than previously thought (Devos 2014a, b; Boedeker et al. 2017).

Despite this recent reinterpretation, Planctomycetes are still extraordinary. They are found in high abundance in biofilms on marine surfaces such as phototrophs (Bengtsson et al. 2012; Bondoso et al. 2014a, b, 2015, 2017; Lage and Bondoso 2014; Vollmers et al. 2017), where they can be the main players in the microbial community (Bengtsson and Øvreås 2010; Kohn et al. 2019). Considering their slow growth compared to natural competitors on nutrient-rich algal surfaces, such as members of the *Roseobacter* clade (Frank et al. 2015; Wiegand et al. 2018), their dominance is remarkable. A possible explanation for this could be the production of yet for the most part uncharacterised small bioactive molecules that could e.g. be involved in mediating symbiotic interactions with algae or that could act as antibiotic agents (Graca et al. 2016; Jeske et al. 2016; Kallscheuer et al. 2019b). During the lifecycle of members of the *Planctomycetaceae*, a typical lifestyle switch can be observed (Jogler et al. 2011; Wiegand et al. 2018). It is hypothesised that in such cases a flagellated swimmer cell responds to an environmental clue, such as the secretion of dissolved organic carbon, and attaches to the phototroph by formation of a holdfast structure (Wiegand et al. 2018). A biofilm can then form, allowing the Planctomycete to degrade complex polysaccharides released by the host phototroph (Jeske et al. 2013; Lachnit et al. 2013).

To extend our knowledge on Planctomycetes, we here characterise the novel planctomycetal strain CA12^T isolated from giant bladder kelp (*Macrocystis pyrifera*) in Monterey Bay, California, USA by using physiological, microscopic, genomic and phylogenetic methods. Based on these analyses, we propose that strain CA12^T represents a novel species of a novel genus within the planctomycetal family *Planctomycetaceae*.

Materials and methods

Isolation and maintenance

M. pyrifera kelp material was collected in Monterey Bay, California, USA on the 28th of September 2014 (sampling location: 36.619 N 121.901 W) as described previously (Vollmers et al. 2017). For the isolation of strain CA12^T kelp pieces were washed with 100 mg l^{-1} cycloheximide solution dissolved in sterile filtrated natural seawater. Afterwards kelp pieces were swabbed over media plates solidified with gellan gum (8 g l^{-1}, autoclaved separately). To select for planctomycetal strains 1000 mg l^{-1} streptomycin and 200 mg l^{-1} ampicillin was added to the isolation medium. To prevent fungal growth

20 mg l^{-1} cycloheximide was added. The medium for isolation consisted of 2.38 g l^{-1} HEPES as buffer and 20 ml l^{-1} mineral salt solution with 10 g l^{-1} nitrilotriacetic acid (NTA), 29.7 g l^{-1} $MgSO_4 \times 7\ H_2O$, 3.34 g l^{-1} $CaCl_2 \times 2\ H_2O$, 0.01267 g l^{-1} $Na_2MoO_4 \times 2\ H_2O$, 0.099 g l^{-1} $FeSO_4 \times 7\ H_2O$ and 50 ml l^{-1} metal salt sol. 44. NTA was dissolved in 700 ml distilled water by adjusting the pH to 7.2 with KOH. All further components were dissolved separately and added slowly. The solution was sterilised by filtration and stored at 4 °C. Metal salt solution 44 consisted of 250 mg l^{-1} Na_2-EDTA, 1095 mg l^{-1} $ZnSO \times 7\ H_2O$, 500 mg l^{-1} $FeSO_4 \times 7\ H_2O$, 154 mg l^{-1} $MnSO_4 \times H_2O$, 39.5 mg l^{-1} $CuSO_4 \times 5\ H_2O$, 20.3 mg l^{-1} $CoCl_2 \times 6\ H_2O$ and 17.7 mg l^{-1} $Na_2B_4O_7 \times 10\ H_2O$. In the first step, EDTA was dissolved and, if required, a few drops of concentrated H_2SO_4 were added to retard precipitation of the heavy metal ions. The solution was sterilised by filtration and stored at 4 °C. Furthermore, the medium was supplemented with 5 ml l^{-1} vitamin solution consisting of 10 mg l^{-1} *p*-aminobenzoic acid, 4 mg l^{-1} biotin, 20 mg l^{-1} pyridoxine hydrochloride, 10 mg l^{-1} thiamine hydrochloride, 10 mg l^{-1} Ca-pantothenate, 4 mg l^{-1} folic acid, 10 mg l^{-1} riboflavin, 10 mg l^{-1} nicotinamide and 0.2 mg l^{-1} vitamin B12. *p*-Aminobenzoic acid was dissolved first, the solution was sterilised by filtration and stored in the dark at 4 °C. In addition, 1 ml l^{-1} trace element solution (1.5 g l^{-1} Na-NTA, 500 mg l^{-1} $MnSO_4 \times H_2O$, 100 mg l^{-1} $FeSO_4 \times 7\ H_2O$, 100 mg l^{-1} $Co(NO_3)_2 \times 6\ H_2O$, 100 mg l^{-1} $ZnCl_2$, 50 mg l^{-1} $NiCl_2 \times 6\ H_2O$, 50 mg l^{-1} H_2SeO_3, 10 mg l^{-1} $CuSO_4 \times 5\ H_2O$, 10 mg l^{-1} $AlK(SO_4)_2 \times 12\ H_2O$, 10 mg l^{-1} H_3BO_3, 10 mg l^{-1} $NaMoO_4 \times 2\ H_2O$ and 10 mg l^{-1} $Na_2WO_4 \times 2\ H_2O$) was added. The solution was sterilised by filtration and stored in the dark at 4 °C. HEPES and mineral salt solution were added before autoclaving, while vitamin and trace element solution were added after autoclaving. Furthermore, the medium was supplemented with 250 ml l^{-1} concentrated artificial sea water (ASW) (46.94 g l^{-1} NaCl, 7.84 g l^{-1} Na_2SO_4, 21.28 g l^{-1} $MgCl_2 \times 6\ H_2O$, 2.86 g l^{-1} $CaCl_2 \times 2\ H_2O$, 0.384 g l^{-1} $NaHCO_3$, 1.384 g l^{-1} KCl, 0.192 g l^{-1} KBr, 0.052 g l^{-1} H_3BO_3, 0.08 g l^{-1} $SrCl_2 \times 6\ H_2O$ and 0.006 g l^{-1} NaF) before autoclaving. During isolation *N*-acetyl glucosamine (NAG) (1 g l^{-1}) served as sole carbon and energy source and the pH was adjusted to 8.0. For maintenance of strain CA12^T the medium was supplemented with 0.25 g l^{-1} glucose, 0.25 g l^{-1} peptone and 0.25 g l^{-1} yeast extract in addition to NAG, while no antibiotics and antifungal reagents were used. The pH was adjusted to 7.5.

Morphological and physiological analysis

Physiological tests were performed in M1H NAG ASW medium composed of 250 ml l^{-1} artificial sea water (ASW), 20 ml l^{-1} Hutner's basal salt solution, 0.25 g l^{-1} peptone, 0.25 g l^{-1} yeast extract, 0.25 g l^{-1} glucose, 1 g l^{-1} NAG, 5 ml l^{-1} vitamin solution, 1 ml l^{-1} trace element solution and buffered with either 100 mM MES (pH 5–6), HEPES (pH 7–8) or CHES (pH 9–10) depending on the desired pH. pH was adjusted by adding the appropriate amount of 5 M KOH. Glucose, NAG, vitamin solution and trace element solution were added after autoclaving.

The pH range and optimum were determined upon inoculating 4.5 ml M1H NAG ASW with 1.5 ml preculture and cultivation at 28 °C and 110 rpm. Growth was assessed by measuring the optical density at 600 nm (OD_{600nm}) for a period of 68 h employing a Varian Cary® 50 UV–Vis Spectrophotometer (Agilent Technologies). Temperature range and optimum were determined upon inoculating 4.5 ml M1H NAG ASW of pH 8.0 with 0.5 ml pre-culture and cultivation at 28 °C and 110 rpm. Growth was assessed by measuring OD_{600nm} for a period of 148 h employing an Ultrospec II photometer (LKB Biochrom).

Microscopy techniques

Phase contrast microscopy was performed employing a Nikon Eclipse Ti inverted microscope with a Nikon N Plan Apochromat λ 100x/1.45 oil objective and a Nikon DS-Ri2 camera objective. Cells were immobilised in a fixed focal plane in MalTek glass bottom dishes (35 mm, No. 1.5) using a 1% agarose cushion. The images were analysed using Nikon NIS-Elements software.

Field emission scanning electron microscopy was performed by fixing bacteria for 1 h on ice with 1% formaldehyde in HEPES buffer (3 mM HEPES, 0.3 mM $CaCl_2$, 0.3 mM $MgCl_2$, 2.7 mM sucrose, pH 6.9), after which they were washed with the same buffer. Cover slips with a diameter of 12 mm were coated with a poly-L-lysine solution (Sigma-Aldrich)

for 10 min, washed with distilled water and air-dried. 50 µl of fixed bacteria solution was placed on a coated cover slip and allowed to settle for 10 min. The cover slips containing the fixed bacteria were fixed in 1% glutaraldehyde in TE buffer (20 mM TRIS, 1 mM EDTA, pH 6.9) for 5 min at room temperature. After this, they were washed twice in TE buffer and dehydrated on ice in a graded series of acetone (10, 30, 50, 70, 90 and 100%) for 10 min in each concentration. After dehydration, the samples were brought to room temperature and placed in fresh 100% acetone. Samples were subsequently subjected to critical point drying with liquid CO_2 (CPD 300, Leica), after which they were covered with an 80/20 gold/palladium film by sputter coating (SCD 500, Bal-Tec). The samples were examined with a field emission scanning electron microscope (Zeiss Merlin) employing the Everhart–Thornley HESE2 detector and the inlens SE detector with a 25:75 ratio and an acceleration voltage of 5 kV.

Transmission electron microscopy (TEM) was performed employing the floating grid method: carbon-coated copper grids were placed on 3 ml of CA12^T culture in M1H NAG ASW medium in a 6-well plate and were incubated for 24 h or 48 h at 28 °C. After this, the grids were negative stained with 0.5% uranyl acetate (UA), by rinsing twice with 0.5% UA followed by 1 min incubation with 0.5% UA and subsequent blotting an air-drying. Micrographs were taken with a JEM 1400 (JEOL) employing an acceleration voltage of 120 kV. Images were captured with a Matataki Flash sCMOS camera (JEOL) using the Jeol TEM Center software (JEOL).

Time-lapse microscopy was performed employing a DMI8 inverted microscope (Leica) with a HC PL APO 100x/1.40 oil objective (Leica) and a DCF9000GT camera (Leica). Dividing CA12^T cells were analysed using CellAsic Onix microfluidic plates, immobilising the cells in a fixed focal plane. Cells were loaded into the microfluidic plate by using the manufacturer's loading protocol (CellASIC) three times consecutively. A constant flow of M1H NAG ASW medium was provided to the cells by applying 27 kPa of pressure. Cells were imaged under a constant flow of medium for up to 30 h and analysed using FIJI (Schindelin et al. 2012).

Phylogenetic analysis

16S rRNA gene phylogeny was computed for strain CA12^T, the type strains of all described planctomycetal species (as of January 2019) and all isolates recently described (Kallscheuer et al. 2019a; Wiegand et al. 2019). An alignment of 16S rRNA gene sequences was made with SINA (Pruesse et al. 2012). Phylogenetic analysis was performed employing a maximum likelihood approach with 1000 bootstraps, the nucleotide substitution model GTR, gamma distribution and estimation of proportion of invariable sites (GTRGAMMAI option) (Stamatakis 2014). The outgroup consisted of three 16S rRNA genes of bacterial strains from the PVC superphylum. The *average amino acid identity* (AAI) was determined with the aai.rb script of the enveomics collection (Rodriguez-R and Konstantinidis 2016) and the *percentage of conserved proteins* (POCP) was calculated as described before (Qin et al. 2014). The *rpoB* gene sequence was taken from the genome annotation and sequence identities were determined as described before (Bondoso et al. 2013) with clustal Omega (Sievers et al. 2011). The *rpoB* alignment and matrix calculation was performed upon extracting only those parts of the sequence that would have been sequenced with the described primer set. For the multi-locus sequence analysis (MLSA) the unique single-copy core genome of all analysed genomes was determined with proteinortho5 (Lechner et al. 2011) with the 'selfblast' option enabled. The protein sequences of the resulting orthologous groups were aligned using MUSCLE v.3.8.31 (Edgar 2004). After clipping, partially aligned *C*- and *N*-terminal regions and poorly aligned internal regions were filtered using Gblocks (Castresana 2000). The final alignment of 216 ubiquitous genes with a combined length of 103,564 conserved amino acid residues was concatenated and clustered using the maximum likelihood method implemented by RaxML (Stamatakis 2014) with the "rapid bootstrap" method and 500 bootstrap replicates. The outgroup consisted of concatenated gene sets from the *Phycisphaera* and *Candidatus* Brocadiaceae.

Genomic analysis

The genome of strain CA12^T was published previously (Wiegand et al. 2019) and is available from NCBI under acc. no. CP036265. The GenBank acc.

no. of the 16S rRNA gene is MK554521. All other genomes were also gathered from NCBI and their accession numbers are given in the corresponding tables. Completeness and contamination of the genomes was determined using CheckM v1.0.131 (Parks et al. 2015). The primary metabolism was analysed by examining locally computed InterProScan (Mitchell et al. 2019) results cross-referenced with information from the UniProt database (UniProt 2019) and BLASTp results of 'typical' protein sequences. The carbohydrate active enzymes were determined by employing dbCAN2 (Zhang et al. 2018), which automatically mines the CAZy database (Lombard et al. 2014).

Results and discussion

Phylogenetic inference

Based on 16S rRNA gene phylogeny and whole genome-based multilocus sequence analysis (MLSA), strain CA12^T clusters within the planctomycetal family *Planctomycetaceae* (Fig. 1). However, the results about the current nearest neighbour are ambiguous, suggesting either *Planctomicrobium piriforme* P3^T (Kulichevskaya et al. 2015) or *Fuerstiella marisgermanici* NH11^T (Kohn et al. 2016) in the 16S rRNA gene and MSLA trees, respectively. However, all phylogenetic markers employed below did not indicate *F. marisgermanici* NH11^T, but instead either *P. piriforme* P3^T or *Rubinisphaera brasiliensis* DSM 5305^T as the current closest relative to strain CA12^T. With 82.3%, strain CA12^T has a high 16S rRNA gene sequence identity to *P. piriforme* P3^T. This value is far below the suggested 94.5% threshold sequence identity for delineation of genera (Yarza et al. 2014), suggesting that strain CA12^T represents a novel genus within the family *Planctomycetaceae*. For Planctomycetes, the use of 16S rRNA gene phylogeny alone has been inconsistent in distinguishing novel species (Kohn et al. 2019). Therefore other phylogenetic markers, such as the RNA polymerase subunit beta (RpoB) gene (Bondoso et al. 2013), *average nucleotide identity* (ANI) (Kim et al. 2014), AAI (Konstantinidis and Tiedje 2005) and POCP (Qin et al. 2014) can be helpful for achieving greater accuracy in resolving the precise phylogenetic affiliation. As was the case for the 16S rRNA gene, *rpoB* has the highest sequence identity to *P. piriforme* P3^T at 72%, while similarities $< 72\%$ indicate a novel genus (Bondoso et al. 2013). With a POCP value of 39.3%, *R. brasiliensis* DSM 5305^T, rather than *P. piriforme*, has the current highest similarity to strain CA12^T, but this still indicates the strain should be placed in a novel genus as the suggested cut-off value for delineation of genera is 50% (Qin et al. 2014). The AAI was highest to *R. brasiliensis* with both one-way AAIs (46.39% and 45.45%) being below the suggested 60% cut-off value for delineation of genera (Luo et al. 2014), thereby again indicating a novel genus. ANI values $< 70\%$ ensure that strain CA12^T and its relatives belong to separate species. Taken together, these different methods suggest that strain CA12^T represents a novel species within a novel genus.

Genomic characteristics

The genome of strain CA12^T is 5,475,215 bp in size and has a G+C content of 70.1%. It contains 4309 protein-coding genes, of which 1801 encode hypothetical proteins. These values correspond to 787 protein-coding genes per Mb and a coding density of 88.1%. Similar to its relatives, the strain lacks any plasmids. When compared to these close relatives (Table 1), it becomes evident that the genome of strain CA12^T is relatively small while having a high G + C content. Due to its smaller genome, strain CA12^T has a lower count of proteins and especially of those proteins annotated as hypothetical. In accordance, the strain's coding density is higher than in its relatives and it carries no giant genes.

Morphology and physiology

Strain CA12^T forms pink colonies on solid medium (Fig. S1A) and is light pink-coloured in liquid medium, where it has a strong tendency to form biofilms, even when shaken in a baffled flask (Fig. S1B). Such biofilms intensely adhere to the glass surface and are difficult to scrape off, indicating the production of an extracellular matrix or fibres that glue cells to each other and to the glass surface. This finding is not surprising as strain CA12^T was obtained from a natural biofilm on the surface of *M. pyrifera*. The morphology of strain CA12^T was determined employing a variety of microscopy techniques. Cells are spherical to ovoid-shaped and are 2.0 $\pm$ 0.2 µm $\times$

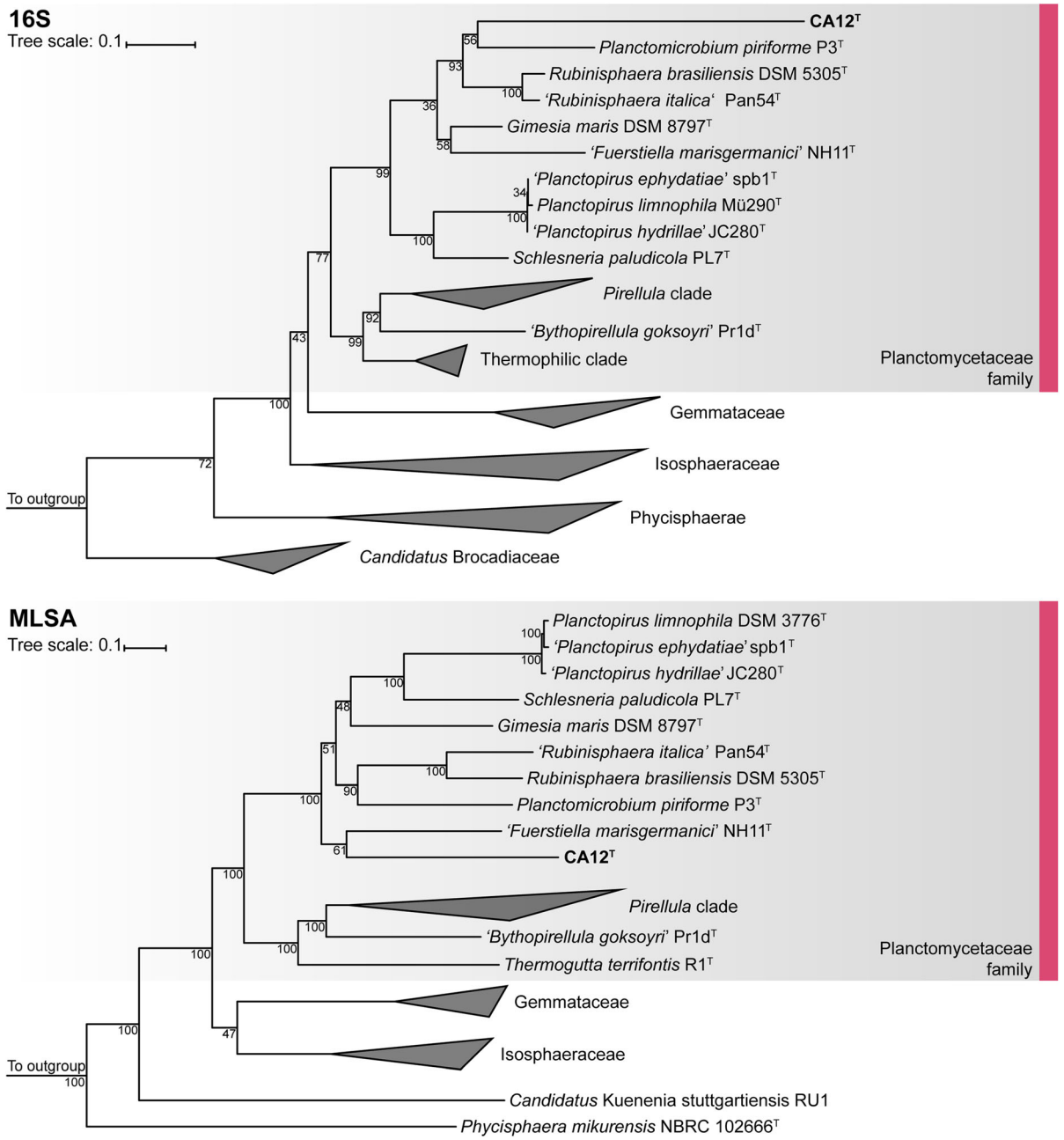

Fig. 1 Phylogenetic trees of the phylum Planctomycetes highlighting the position of strain CA12^T. 16S rRNA gene phylogeny (top panel) and whole genome-based MLSA (bottom panel) were computed using the maximum likelihood method. Bootstrap values after 1000 (16S) or 500 (MLSA) re-samplings are given at the nodes. The outgroups consist of three 16S rRNA genes from the PVC superphylum (top panel) and sequences from strains belonging to the Phycisphaera and *Candidatus* Brocadiaceae (in the MLSA tree)

1.5 ± 0.3 μm in size (Fig. 2a–c). The cell surface is evenly covered with large crateriform structures, with the exception of the pole at which the flagellum is located (Fig. 2g). Strain CA12^T produces a large amount of fibres, which often seem to originate from these crateriform structures. The quantity of fibres is most likely associated with the tendency to form biofilms and to grow in large aggregates (Fig. 2d).

Table 1 Genome features of strain CA12^T compared to the closest related genera

	CA12^T	*Planctomicrobium piriforme* DSM 26348^T*	*Rubinisphaera brasiliensis* DSM 5305^T**	*Gimesia maris* DSM 8797^T***	*Fuerstiella marisgermanici* NH11^T****
Genome size (bp)	5,475,215	6,317,004	6,006,602	7,816,689	8,920,478
GC content	70.7	58.8 (± 1.7)	56.4	50.4	55.9
Total genes (per Mb)	4382 (800)	5117 (810)	4887 (814)	6062 (776)	6732 (755)
tRNAs	65	53	50	66	60
rRNAs (23S–16S–5S)	2–2–2	1–1–1	2–2–2	2–2–1	2–2–1
Total proteins (per Mb)	4309 (787)	5050 (799)	4824 (803)	5986 (766)	6645 (745)
Hypothetical proteins	1798	2814	2581	2400	3890
Coding density	88.51	85.76	86.15	86.89	87.55
Transposable elements	1	1	3	4	2
Giant genes	0	1	0	8	8
Genome status	Closed	Draft (41)	Closed	Closed	Closed
N50 (scaffolds)	5,475,215	263,811	6,006,602	7,816,689	8,920,478
Completeness	94.83	95.69	94.83	98.28	95.69
Contamination	0	1.72	3.45	1.72	1.72

*Genomic data from GenBank acc. no. NZ_FOQD00000000

**Genomic data from GenBank acc. no. CP002546

***Genomic data from GenBank acc. no. CP042910

****Genomic data from GenBank acc. no. CP017641

Furthermore, cells seem to secrete an extracellular matrix, further stabilising the biofilm (Fig. 2d, e). No holdfast structure was observed during electron microscopic analysis.

As found for all members of the family *Planctomycetaceae*, strain CA12^T divides through polar budding (Fig. 2a). Interestingly, the strain seems to form buds while the mother cell itself is still attached to its mother cell. This process of "consecutive budding" was found both in TEM (Fig. 2f) and in time-lapse microscopy experiments (Fig. 3; Movie S1) and has to our knowledge not been described before for members of *Planctomycetaceae*. It leads to the formation of short filaments, containing at least three cells (Fig. S2). Filament formation and multicellularity were described earlier for *Isosphaera pallida* (Giovannoni et al. 1987). In contrast to strain CA12^T, *I. pallida* grows exclusively as filaments and intercalary bud formation always occurs on the chain axis (Giovannoni et al. 1987). The observed short filaments of strain CA12^T always elongate via budding of the terminal cell. Whether strain CA12^T is an intermediate form between filamentous and unicellular growth requires additional attention, but exceeds the scope of this study. In the light of the greater phylogenetic distance to *I. pallida*, a separate development appears more likely (Fig. 1). Nevertheless, future studies on strain CA12^T should address this unusual cell division as a potential progenitor to planctomycetal filament formation.

Compared to its closest related strains, strain CA12^T is of similar size and shape (Table 2). While the mode of division and the shape of the bud are very similar, strain CA12^T is unique compared to its relatives in not having to fulfil a lifestyle switch in order to divide (Table 2). In addition, no stalk or holdfast structure was observed while both are present in *P. piriforme, R. brasiliensis* and *Gimesia maris* (Table 2). All four strains have a flagellum and produce fibres. No capsule could be observed for these strains.

Strain CA12^T cells are capable of growth between 10 and 40 °C with optimal growth at 27 °C and between pH 5.0 and 9.0 with optimal growth at pH 7.5

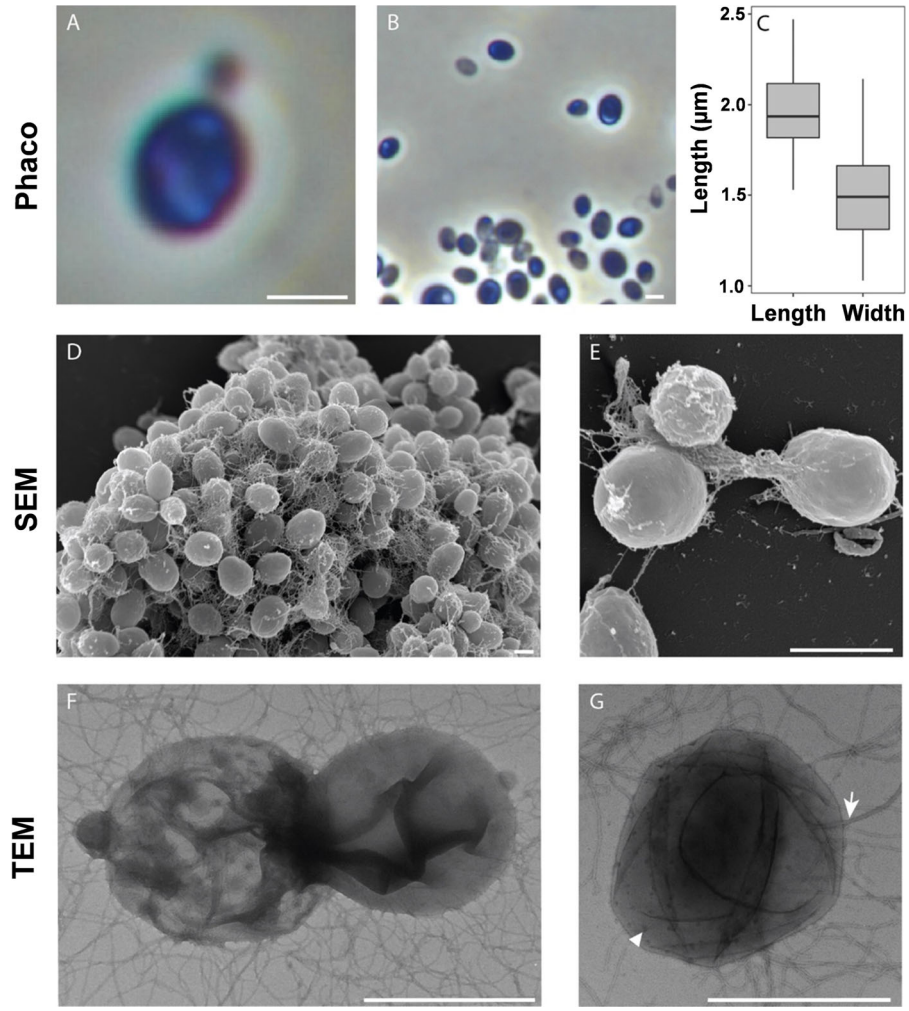

Fig. 2 Morphology of strain CA12^T. Morphology of strain CA12^T is shown by phase contrast (Phaco) microscopy (**a**, **b**), scanning electron microscopy (SEM) (**d**, **e**) and transmission electron microscopy (TEM) (**f**, **g**). Cells divide by polar budding (**a**) and mostly grow in dense aggregates (**d**). Large amounts of fibers are produced and seem to originate from large crateriform structures (**g**, white arrowhead), which evenly cover the cell surface except for the pole at which the flagellum (**g**, white arrow) is located. Cell size of the strain was determined from Phaco images (**c**). Scale bar 1 µm

(Fig. 4). The strain reached a maximal growth rate of 0.065 h^{-1} corresponding to a generation time of approximately 11 h, which is within the range of 0.01–0.09 h^{-1} (generation time of 8–70 h) which we and others have observed for most of the Planctomycetes cultivated so far (Tekniepe et al. 1981; Giovannoni et al. 1987; Kulichevskaya et al. 2008; Bondoso et al. 2014a, b; Kohn et al. 2016). A generation time of 11 h is rather long compared to other bacteria that compete with strain CA12^T for its ecological niche in kelp biofilms. The genome of strain CA12^T was previously found to harbour small molecule biosynthesis-related genes and gene clusters (Wiegand et al. 2019). Thus, the newly discovered strain might be a good candidate for further examination of the planctomycetal chemical interaction in marine biofilms. This might also be true with regard to the strain's primary metabolism (Table 3). All close relatives are predicted to be able to convert glucose via the pentose phosphate pathway as well as by glycolysis via the Entner–Doudoroff (KDPG) and the Embden–Meyerhof–Parnas pathway. While strain

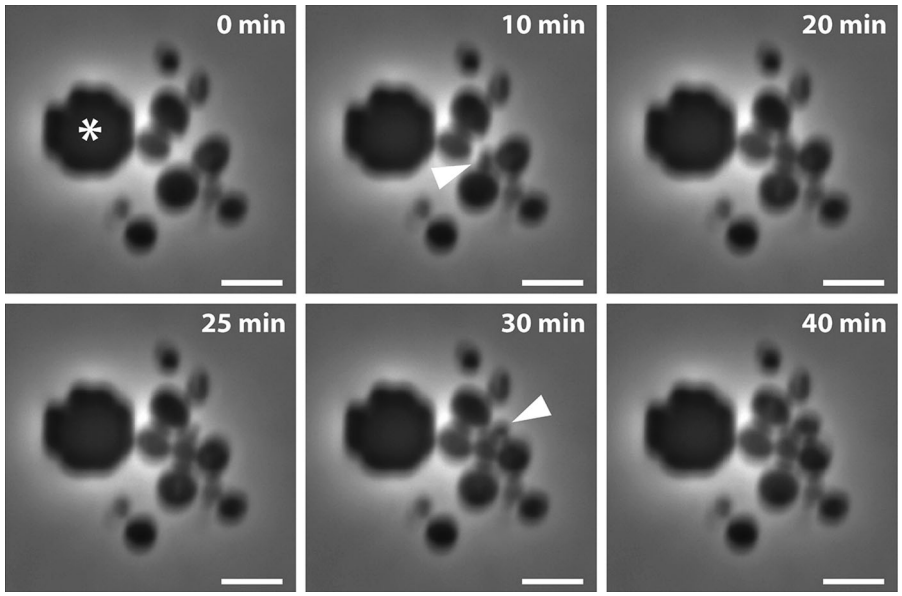

Fig. 3 Phase contrast wide field time-lapse microscopy of strain CA12^T showing consecutive cell division by polar budding. Cells can be seen dividing consecutively by polar budding (white arrowhead). Over time, the same cell undergoes two budding cycles without entirely detaching from the initial mother cell. White asterisk shows microfluidic plate structural pillar. Scale bar 1 μm

CA12^T possesses the genes for the pentose phosphate pathway, it lacks the genes for the KDPG pathway. Interestingly, it also seems to lack *pgk*, which encodes phosphoglycerate kinase converting 1,3-bisphosphoglycerate to 3-phosphoglycerate. We identified some aldehyde dehydrogenases that might be able to bypass this reaction by converting glyceraldehyde-3-phosphate directly to 3-phosphoglycerate but it requires further analyses to investigate this hypothesis. During gluconeogenesis, strain CA12^T seems to depend on GTP (instead of ATP as in its relatives) to convert oxaloacetate to phosphoenolpyruvate. All compared strains appear to possess the expected enzymes for the citric acid cycle (TCA cycle), but all lack the glyoxylate shunt. In terms of its carbohydrate-degrading potential, CA12^T has slightly less enzymes than its close relatives, potentially due to the smaller genome (Table 4). However, the number of glycosyltransferases exceeds the number present in close relatives, pointing towards different nutritional sources of the different strains.

Description of *Alienimonas* gen. nov.

Alienimonas (*A.li.e.ni.mon'as.* L. masc. adj. *alienus* strange, foreign; Gr. fem. n. *monas* a unit, monad; N.L. fem. n. *Alienimonas* an alien bacterial unit).

Members of the genus are Gram-negative, aerobic, mesophilic, neutrophilic and heterotrophic. Cells are spherical to ovoid-shaped, divide by polar budding and produce fibres originating from large crateriform structures. The type species of the genus is *Alienimonas californiensis*.

Description of *Alienimonas californiensis* sp. nov.

Alienimonas californiensis (ca.*li.for.ni.en'sis*. N.L. fem. adj. *californiensis* of California; referring to the isolation of the type strain from California).

In addition to the general characteristics of the genus, cells are 2.0 ± 0.2 μm $\times$ 1.5 ± 0.2 μm in size. They form pink colonies and have a strong tendency to form aggregates and biofilms. Cells divide

Table 2 Phenotypic features of strain CA12^T compared to the closest related genera

	CA12^T	*Planctomicrobium piriforme* DSM 26348^T*	*Rubinisphaera brasiliensis* DSM 5305^T**	*Gimesia maris* DSM 8797^T***	*Fuerstiella marisgermanici* NH11^T****
Shape	Spherical to ovoid	Ellipsoidal to pear-shaped	Spherical to ovoid	Spherical to ovoid	Ovoid, pear-shaped
Cell size	2.0 ± 0.2 µm × 1.5 ± 0.3 µm	1.7–2.8 µm × 0.9–1.3 µm	0.7–1.8 µm	0.4–1.5	1.2–2.5 × 0.9–1.7
Aggregates	Yes	Rosettes	Yes and rosettes	n. d.	Yes
Crateriform structures	Evenly covered, except for the pole at which the flagellum is located	Polar	Whole cell surface	n. d.	Reproductive pole
Budding pole	Polar	Polar, opposite pole at which stalk is located	Polar, opposite pole at which stalk is located	Polar, opposite pole at which stalk is located	Polar
Cell cycle	No	Yes	Yes	Yes	Yes
Stalk	n.o.	Yes	Yes	Yes	n.o.
Holdfast structure	n.o.	Yes	Yes	Yes	n.o.

n.d. not determined; *n.o.* not observed

*Phenotypic data from (Kulichevskaya et al. 2015)

**Phenotypic data from (Schlesner 1989)

***Phenotypic data from (Bauld and Staley 1976)

****Phenotypic data from (Kohn et al. 2016)

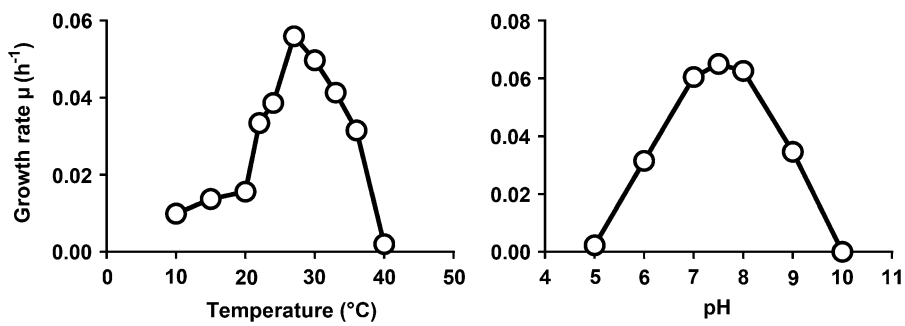

Fig. 4 Temperature and pH optimum of strain CA12^T. Cultivations were performed as described in the Materials and methods section

by polar budding and have the ability to perform this consecutively, without fulfilling a lifestyle switch. The outer membrane is evenly covered with large crateriform structures, except near the pole where the flagellum is located. Fibres originating from crateriform structures are observed. Cells grow between pH 5.0 and 9.0 with optimal growth at pH 7.5 and between 10 and 40 °C with optimal growth at 27 °C. The G + C content of the type strain is 70.1%. The 5.5 Mb genome (acc. no. CP036265) and 16S rRNA gene (acc. no. MK554521) sequences of the type strain have been deposited at GenBank.

Table 3 Genome-based primary metabolism of strain CA12^T compared to the closest related genera

Reaction/enzyme	EC number	Gene	CA12^T	*Planctomicrobium piriforme* DSM 26348^T*	*Rubinisphaera brasiliensis* DSM 5305^T**	*Gimesia maris* DSM 8797^T***	*Fuerstiella marisgermanici* NH11^T****
Glycolysis (Embden–Meyerhof–Parnas pathway)							
Glucose-6-phosphate isomerase	5.3.1.9	*pgi*	CA12_32240	y	y	y	y
ATP-dependent 6-phosphofructokinase isozyme 1	2.7.1.11	*pfkA*	CA12_14770	y	y	y	y
Fructose-bisphosphate aldolase class 2	4.1.2.13	*fbaA*	CA12_43320	y	y	y	y
Triosephosphate isomerase	5.3.1.1	*tpiA*	CA12_39850	y	y	y	y
Glyceraldehyde-3-phosphate dehydrogenase	1.2.1.12	*gapA*	CA12_36350	y	y	y	y
Phosphoglycerate kinase	2.7.2.3	*pgk*	n	y	y	y	y
NAD(P)-dependent glyceraldehyde-3-phosphate dehydrogenase	1.2.1.90/ 1.2.1.9	*gapN*	Candidates	Candidates	Candidates	Candidates	Candidates
2,3-Bisphosphoglycerate-dependent phosphoglycerate mutase	5.4.2.11	*gpmA*	CA12_30720	y	y	y	y
Enolase	4.2.1.11	*eno*	CA12_00460	y	y	y	y
Pyruvate kinase I	2.7.1.40	*pykF*	CA12_30440	y	y	y	y
Pyruvate dehydrogenase complex	1.2.4.1/ 2.3.1.12	*aceEF*	CA12_20210/CA12_20200	y	y	y	y
Gluconeogenesis							
Pyruvate, phosphate dikinase	2.7.9.1	*ppdK*	CA12_36740	y	y	y	y
Phosphoenolpyruvate carboxykinase (ATP)	4.1.1.49	*pckA*	n	y	y	y	y
Phosphoenolpyruvate carboxykinase [GTP]	4.1.1.32	*pckG*	CA12_16520	n	n	n	n
Pyrophosphate–fructose 6-phosphate 1-phosphotransferase	2.7.1.90	*pfp*	CA12_41240	y	y	y	y
Pentose phosphate pathway							
Glucose-6-phosphate 1-dehydrogenase	1.1.1.49	*zwf*	CA12_01770	y	y	y	y
6-Phosphogluconolactonase	3.1.1.31	*pgl*	CA12_42430	y	y	y	y
6-Phosphogluconate dehydrogenase	1.1.1.44	*gndA*	CA12_41200	y	y	y	y
Transketolase	2.2.1.1	*tkt*	CA12_17310	y	y	y	y
Transaldolase	2.2.1.2	*tal*	CA12_24580	y	y	y	y
KDPG (Entner–Doudoroff) pathway							
KDPG aldolase	4.1.2.14	*eda*	n	y	y	y	y

Table 3 continued

Reaction/enzyme	EC number	Gene	CA12^T	*Planctomicrobium piriforme* DSM 26348^T*	*Rubinisphaera brasiliensis* DSM 5305^T**	*Gimesia maris* DSM 8797^T***	*Fuerstiella marisgermanici* NH11^T****
Phosphogluconate dehydratase	4.2.1.12	*edd*	n	y	y	y	y
TCA cycle							
Citrate synthase	2.3.3.16	*gltA*	CA12_00670	y	y	y	y
Aconitate hydratase A	4.2.1.3	*acnA*	CA12_34980	y	y	y	y
Isocitrate dehydrogenase [NADP]	1.1.1.42	*icd*	CA12_15100	y	y	y	n
Isocitrate–homoisocitrate dehydrogenase	1.1.1.286		CA12_34890	y	y	y	y
2-Oxoglutarate dehydrogenase complex	1.2.4.2/ 2.3.1.61	*sucAB*	CA12_20480/CA12_13510	y	y	y	y
Succinate–CoA ligase complex	6.2.1.5	*sucCD*	CA12_41420/CA12_41410	y	y	y	y
Succinate dehydrogenase complex	1.3.5.1	*sdhABC*	CA12_39470/CA12_39480/ CA12_39460	y	y	y	y
Fumarate hydratase	4.2.1.2	*fumC*	CA12_01380	y	y	y	y
Malate dehydrogenase	1.1.1.37	*mdh*	CA12_04080	y	y	y	y

For strain CA12^T the locus tag is given whenever a gene was identified. Presence of a gene in the other strains is indicated by 'y' and absence is indicated by 'n'. When different enzymes are capable of performing a reaction, the enzymes are not separated by an underline. In case of EC 1.2.1.90 and EC 1.2.1.9 several aldehyde dehydrogenases were identified ('candidates')

*Genomic data from GenBank acc. no. NZ_FOQD00000000

**Genomic data from GenBank acc. no. CP002546

***Genomic data from GenBank acc. no. CP042910

****Genomic data from GenBank acc. no. CP017641

Table 4 Carbohydrate-degrading enzymes of strain CA12^T compared to the closest related genera

	CA12^T	*Planctomicrobium piriforme* DSM 26348^T*	*Rubinisphaera brasiliensis* DSM 5305^T**	*Gimesia maris* DSM 8797^T***	*Fuerstiella marisgermanici* NH11^T****
Carbohydrate esterases	26	41	37	56	60
Glycoside hydrolases	56	61	55	78	83
Glycosyltransferases	77	56	75	60	70
Polysaccharide lyases	5	2	3	5	5
Carbohydrate-binding	19	27	34	50	58
Auxiliary activities	2	4	2	3	4
Unknown	3	4	3	5	6

*Genomic data from GenBank acc. no. NZ_FOQD00000000

**Genomic data from GenBank acc. no. CP002546

***Genomic data from GenBank acc. no. CP042910

****Genomic data from GenBank acc. no. CP017641

The type strain, CA12^T (DSM 100707^T = LMG 29076^T), was isolated from *Macrocystis pyrifera* in Monterey Bay, California, USA.

Acknowledgements We thank Anne-Kristin Kaster (KIT Karlsruhe, Germany) and Alfred M. Spormann (Stanford, USA) as well as the Aquarius Dive Shop Monterey and the Hopkins Marine Station for sampling support. We further thank Ina Schleicher for excellent SEM sample preparation and skillful technical assistance and the General Instrumentation department at Radboud University for help during the TEM analyses. For their support during strain deposition we thank the BCCM/LMG bacteria collection and Brian Tindall and Regine Fähnrich from the DSMZ.

Author contributions ASB performed cultivations and wrote the manuscript; NK contributed to preparation of the text, analyzed the data and prepared the figures; SW and MJ performed the genomic and phylogenetic analysis; PR and AH isolated the strain and performed the initial strain cultivation and deposition; SHP and CB performed the light microscopic analysis; RJM performed the transmission electron microscopy; MSMJ contributed to text preparation and revised the manuscript; MR performed the electron microscopic analysis; CJ and MJ took the samples in Monterey Bay, CA; CJ supervised the study and all authors read and approved the final version of the manuscript.

Funding This work was funded by the Deutsche Forschungsgemeinschaft (DFG) grants KA 4967/1-1 and JO 893/4-1, and by the grant ALWOP.308 of the Nederlandse Organisatie voor Wetenschappelijk Onderzoek (NWO).

Compliance with ethical standards

Conflict of interest The authors declare that they have no conflict of interest.

Ethical statement This article does not contain any studies with animals performed by any of the authors.

References

Acehan D, Santarella-Mellwig R, Devos DP (2014) A bacterial tubulovesicular network. J Cell Sci 127:277–280

Bauld J, Staley JT (1976) *Planctomyces maris* sp. nov.: a marine isolate of the *Planctomyces-Blastocaulis* group of budding bacteria. J Gen Microbiol 97:45–55

Bengtsson MM, Øvreås L (2010) Planctomycetes dominate biofilms on surfaces of the kelp *Laminaria hyperborea*. BMC Microbiol 10:261

Bengtsson MM, Sjøtun K, Lanzén A, Øvreås L (2012) Bacterial diversity in relation to secondary production and succession on surfaces of the kelp *Laminaria hyperborea*. ISME J 6:2188

Boedeker C, Schüler M, Reintjes G, Jeske O, van Teeseling MC, Jogler M, Rast P, Borchert D, Devos DP, Kucklick M (2017) Determining the bacterial cell biology of Planctomycetes. Nat Commun 8:14853

Bondoso J, Harder J, Lage OM (2013) *rpoB* gene as a novel molecular marker to infer phylogeny in Planctomycetales. Antonie Van Leeuwenhoek 104:477–488

Bondoso J, Balagué V, Gasol JM, Lage OM (2014a) Community composition of the Planctomycetes associated with different macroalgae. FEMS Microbiol Ecol 88:445–456

Bondoso J, Albuquerque L, Lobo-da-Cunha A, Da Costa MS, Harder J, Lage OM (2014b) *Rhodopirellula lusitana* sp. nov. and *Rhodopirellula rubra* sp. nov., isolated from the surface of macroalgae. Syst Appl Microbiol 37:157–164

Bondoso J, Albuquerque L, Nobre MF, Lobo-da-Cunha A, da Costa MS, Lage OM (2015) *Roseimaritima ulvae* gen. nov., sp. nov. and *Rubripirellula obstinata* gen. nov., sp. nov. two novel Planctomycetes isolated from the epiphytic community of macroalgae. Syst Appl Microbiol 38:8–15

Bondoso J, Godoy-Vitorino F, Balagué V, Gasol JM, Harder J, Lage OM (2017) Epiphytic Planctomycetes communities associated with three main groups of macroalgae. FEMS Microbiol Ecol 93:fiw255

Castresana J (2000) Selection of conserved blocks from multiple alignments for their use in phylogenetic analysis. Mol Biol Evol 17:540–552

Devos DP (2014a) PVC bacteria: variation of, but not exception to, the Gram-negative cell plan. Trends Microbiol 22:14–20

Devos DP (2014b) Re-interpretation of the evidence for the PVC cell plan supports a Gram-negative origin. Antonie Van Leeuwenhoek 105:271–274

Devos DP, Jogler C, Fuerst JA (2013) The 1st EMBO workshop on PVC bacteria-Planctomycetes-Verrucomicrobia-Chlamydiae superphylum: exceptions to the bacterial definition? Antonie Van Leeuwenhoek 104:443–449

Edgar RC (2004) MUSCLE: multiple sequence alignment with high accuracy and high throughput. Nucleic Acids Res 32:1792–1797

Frank O, Michael V, Pauker O, Boedeker C, Jogler C, Rohde M, Petersen J (2015) Plasmid curing and the loss of grip—the 65-kb replicon of *Phaeobacter inhibens* DSM 17395 is required for biofilm formation, motility and the colonization of marine algae. Syst Appl Microbiol 38:120–127

Fuerst JA, Sagulenko E (2011) Beyond the bacterium: Planctomycetes challenge our concepts of microbial structure and function. Nat Rev Microbiol 9:403

Fuerst JA, Webb RI (1991) Membrane-bounded nucleoid in the eubacterium *Gemmatata obscuriglobus*. Proc Natl Acad Sci USA 88:8184–8188

Fukunaga Y, Kurahashi M, Sakiyama Y, Ohuchi M, Yokota A, Harayama S (2009) *Phycisphaera mikurensis* gen. nov., sp. nov., isolated from a marine alga, and proposal of Phycisphaeraceae fam. nov., Phycisphaerales ord. nov. and Phycisphaerae classis nov. in the phylum Planctomycetes. J Gen Appl Microbiol 55:267–275

Giovannoni S, Schabtach E, Castenholz RW (1987) *Isosphaera pallida*, gen. and comb. nov., a gliding, budding eubacterium from hot springs. Arch Microbiol 147:276–284

Graca AP, Calisto R, Lage OM (2016) Planctomycetes as novel source of bioactive molecules. Front Microbiol 7:16

Jeske O, Jogler M, Petersen J, Sikorski J, Jogler C (2013) From genome mining to phenotypic microarrays: Planctomycetes as source for novel bioactive molecules. Antonie Van Leeuwenhoek 104:551–567

Jeske O, Schüler M, Schumann P, Schneider A, Boedeker C, Jogler M, Bollschweiler D, Rohde M, Mayer C, Engelhardt H (2015) Planctomycetes do possess a peptidoglycan cell wall. Nat Commun 6:7116

Jeske O, Surup F, Ketteniß M, Rast P, Förster B, Jogler M, Wink J, Jogler C (2016) Developing techniques for the utilization of Planctomycetes as producers of bioactive molecules. Front Microbiol 7:1242

Jogler C (2014) The bacterial 'mitochondrium'. Mol Microbiol 94:751–755

Jogler C, Glockner FO, Kolter R (2011) Characterization of *Planctomyces limnophilus* and development of genetic tools for its manipulation establish it as a model species for the phylum Planctomycetes. Appl Envrion Microbiol 77:5826–5829

Kallscheuer N, Jogler M, Wiegand S, Peeters S, Heuer A, Boedeker C, Jetten MSM, Rohde M, Jogler C (2019a) *Rubinisphaera italica* sp. nov. isolated from a hydrothermal area in the Tyrrhenian Sea close to the volcanic island Panarea. Antonie Van Leeuwenhoek. https://doi.org/10.1007/s10482-019-01329-w

Kallscheuer N, Moreira C, Airs R, Llewellyn CA, Wiegand S, Jogler C, Lage OM (2019b) Pink-and orange-pigmented Planctomycetes produce saproxanthin-type carotenoids including a rare C45 carotenoid. Environ Microbiol Rep 11:741–748

Kim M, Oh HS, Park SC, Chun J (2014) Towards a taxonomic coherence between average nucleotide identity and 16S rRNA gene sequence similarity for species demarcation of prokaryotes. Int J Syst Evol Microbiol 64:346–351

Kohn T, Heuer A, Jogler M et al (2016) *Fuerstia marisgermanicae* gen. nov., sp nov., an unusual member of the phylum Planctomycetes from the German Wadden Sea. Front Microbiol 7:15

Kohn T, Wiegand S, Boedeker C, Rast P, Heuer A, Jetten MSM, Schüler M, Becker S, Rohde C, Müller R-W, Brümmer F, Rohde M, Engelhardt H, Jogler M, Jogler C (2019) *Planctopirus ephydatiae*, a novel Planctomycete isolated from a freshwater sponge. Syst Appl Microbiol. https://doi.org/10.1016/j.syapm.2019.126022

König E, Schlesner H, Hirsch P (1984) Cell wall studies on budding bacteria of the *Planctomyces/Pasteuria* group and on a *Prosthecomicrobium* sp. Arch Microbiol 138:200–205

Konstantinidis KT, Tiedje JM (2005) Towards a genome-based taxonomy for prokaryotes. J Bacteriol 187:6258–6264

Kovaleva O, Merkel AY, Novikov A, Baslerov R, Toshchakov S, Bonch-Osmolovskaya E (2015) *Tepidisphaera mucosa* gen. nov., sp. nov., a moderately thermophilic member of the class Phycisphaerae in the phylum Planctomycetes, and proposal of a new family, Tepidisphaeraceae fam. nov., and a new order, Tepidisphaerales ord. nov. Int J Syst Evol Microbiol 65:549–555

Kulichevskaya IS, Ivanova AO, Baulina OI, Bodelier PL, Damste JSS, Dedysh SN (2008) *Singulisphaera acidiphila* gen. nov., sp. nov., a non-filamentous, Isosphaera-like Planctomycete from acidic northern wetlands. Int J Syst Evol Microbiol 58:1186–1193

Kulichevskaya IS, Ivanova AA, Detkova EN, Rijpstra WI, Sinninghe Damste JS, Dedysh SN (2015) *Planctomicrobium piriforme* gen. nov., sp. nov., a stalked Planctomycete from a littoral wetland of a boreal lake. Int J Syst Evol Microbiol 65:1659–1665

Kulichevskaya IS, Ivanova AA, Suzina NE, Rijpstra WIC, Damste JSS, Dedysh SN (2016) *Paludisphaera borealis* gen. nov., sp. nov., a hydrolytic Planctomycete from northern wetlands, and proposal of Isosphaeraceae fam. nov. Int J Syst Evol Microbiol 66:837–844

Kulichevskaya IS, Ivanova AA, Baulina OI, Rijpstra WIC, Damsté JSS, Dedysh SN (2017) *Fimbriiglobus ruber* gen. nov., sp. nov., a Gemmata-like Planctomycete from Sphagnum peat bog and the proposal of Gemmataceae fam. nov. Int J Syst Evol Microbiol 67:218–224

Lachnit T, Fischer M, Kunzel S, Baines JF, Harder T (2013) Compounds associated with algal surfaces mediate epiphytic colonization of the marine macroalga *Fucus vesiculosus*. FEMS Microbiol Ecol 84:411–420

Lage OM, Bondoso J (2014) Planctomycetes and macroalgae, a striking association. Front Microbiol 5:267

Lechner M, Findeiss S, Steiner L, Marz M, Stadler PF, Prohaska SJ (2011) Proteinortho: detection of (co-)orthologs in large-scale analysis. BMC Bioinform 12:124

Lindsay MR, Webb RI, Fuerst JA (1997) Pirellulosomes: a new type of membrane-bounded cell compartment in Planctomycete bacteria of the genus *Pirellula*. Microbiology-UK 143:739–748

Lombard V, Golaconda Ramulu H, Drula E, Coutinho PM, Henrissat B (2014) The carbohydrate-active enzymes database (CAZy) in 2013. Nucleic Acids Res 42:D490–D495

Lonhienne TG, Sagulenko E, Webb RI, Lee KC, Franke J, Devos DP, Nouwens A, Carroll BJ, Fuerst JA (2010) Endocytosis-like protein uptake in the bacterium *Gemmata obscuriglobus*. Proc Natl Acad Sci USA 107:12883–12888

Luo C, Rodriguez-R LM, Konstantinidis KT (2014) MyTaxa: an advanced taxonomic classifier for genomic and metagenomic sequences. Nucleic Acids Res 42:e73–e73

Mitchell AL, Attwood TK, Babbitt PC et al (2019) InterPro in 2019: improving coverage, classification and access to protein sequence annotations. Nucleic Acids Res 47:D351–D360

Neumann S, Wessels H, Rijpstra WIC, Damste JSS, Kartal B, Jetten MSM, van Niftrik L (2014) Isolation and characterization of a prokaryotic cell organelle from the anammox bacterium *Kuenenia stuttgartiensis*. Mol Microbiol 94:794–802

Parks DH, Imelfort M, Skennerton CT, Hugenholtz P, Tyson GW (2015) CheckM: assessing the quality of microbial genomes recovered from isolates, single cells, and metagenomes. Genome Res 25:1043–1055

Peeters SH, van Niftrik L (2019) Trending topics and open questions in anaerobic ammonium oxidation. Curr Opin Chem Biol 49:45–52

Pruesse E, Peplies J, Glöckner FO (2012) SINA: accurate high-throughput multiple sequence alignment of ribosomal RNA genes. Bioinformatics 28:1823–1829

Qin Q-L, Xie B-B, Zhang X-Y, Chen X-L, Zhou B-C, Zhou J, Oren A, Zhang Y-Z (2014) A proposed genus boundary for the prokaryotes based on genomic insights. J Bacteriol 196:2210–2215

Rast P, Glockner I, Boedeker C et al (2017) Three novel species with peptidoglycan cell walls form the new genus *Lacunisphaera* gen. nov in the family Opitutaceae of the Verrucomicrobial subdivision 4. Front Microbiol 8:18

Rivas-Marin E, Canosa I, Santero E, Devos DP (2016) Development of genetic tools for the manipulation of the Planctomycetes. Front Microbiol 7:10

Rodriguez-R LM & Konstantinidis KT (2016) The enveomics collection: a toolbox for specialized analyses of microbial genomes and metagenomes. *PeerJ Preprints*

Santarella-Mellwig R, Pruggnaller S, Roos N, Mattaj IW, Devos DP (2013) Three-dimensional reconstruction of bacteria with a complex endomembrane system. PLoS Biol 11:9

Scheuner C, Tindall BJ, Lu M, Nolan M, Lapidus A, Cheng J-F, Goodwin L, Pitluck S, Huntemann M, Liolios K (2014) Complete genome sequence of *Planctomyces brasiliensis* type strain (DSM 5305 T), phylogenomic analysis and reclassification of Planctomycetes including the descriptions of *Gimesia* gen. nov., *Planctopirus* gen. nov. and *Rubinisphaera* gen. nov. and emended descriptions of the order Planctomycetales and the family Planctomycetaceae. Stand Genomic Sci 9:10

Schindelin J, Arganda-Carreras I, Frise E, Kaynig V, Longair M, Pietzsch T, Preibisch S, Rueden C, Saalfeld S, Schmid B (2012) Fiji: an open-source platform for biological-image analysis. Nat Methods 9:676

Schlesner H (1989) *Planctomyces brasiliensis* sp. nov., a halotolerant bacterium from a salt pit. Syst Appl Microbiol 12:159–161

Sievers F, Wilm A, Dineen D, Gibson TJ, Karplus K, Li W, Lopez R, McWilliam H, Remmert M, Söding J (2011) Fast, scalable generation of high-quality protein multiple sequence alignments using Clustal Omega. Mol Syst Biol 7:539

Spring S, Bunk B, Spröer C, Rohde M, Klenk HP (2018) Genome biology of a novel lineage of Planctomycetes widespread in anoxic aquatic environments. Environ Microbiol 20:2438–2455

Stamatakis A (2014) RAxML version 8: a tool for phylogenetic analysis and post-analysis of large phylogenies. Bioinformatics 30:1312–1313

Tekniepe BL, Schmidt JM, Starr P (1981) Life cycle of a budding and appendaged bacterium belonging to morphotype IV of the Blastocaulis-Planctomyces group. Curr Microbiol 5:1–6

UniProt C (2019) UniProt: a worldwide hub of protein knowledge. Nucleic Acids Res 47:D506–D515

van Teeseling MCF, Mesman RJ, Kuru E, Espaillat A, Cava F, Brun YV, VanNieuwenhze MS, Kartal B, van Niftrik L (2015) Anammox Planctomycetes have a peptidoglycan cell wall. Nat Commun 6:6

Vollmers J, Frentrup M, Rast P, Jogler C, Kaster A-K (2017) Untangling genomes of novel planctomycetal and verrucomicrobial species from Monterey Bay kelp forest metagenomes by refined binning. Front Microbiol 8:472

Wagner M, Horn M (2006) The Planctomycetes, Verrucomicrobia, Chlamydiae and sister phyla comprise a superphylum with biotechnological and medical relevance. Curr Opin Biotechnol 17:241–249

Wiegand S, Jogler M, Jogler C (2018) On the maverick Planctomycetes. FEMS Microbiol Rev 42:739–760

Wiegand S, Jogler M, Boedeker C, Pinto D, Vollmers J, Rivas-Marín E, Kohn T, Peeters SH, Heuer A, Rast P, Oberbeckmann S, Bunk B, Jeske O, Meyerdierks A, Storesund JE, Kallscheuer N, Lücker S, Lage OM, Pohl T, Merkel BJ, Hornburger P, Müller R-W, Brümmer F, Labrenz M, Spormann AM, Op den Camp HJM, Overmann J, Amann R, Jetten MSM, Mascher T, Medema MH, Devos DP,

Kaster A-K, Øvreås L, Rohde M, Galperin MY, Jogler C (2019) Cultivation and functional characterization of 79 Planctomycetes uncovers their unique biology. Nat Microbiol. https://doi.org/10.1038/s41564-019-0588-1

Yarza P, Yilmaz P, Pruesse E, Glöckner FO, Ludwig W, Schleifer K-H, Whitman WB, Euzéby J, Amann R, Rosselló-Móra R (2014) Uniting the classification of cultured and uncultured bacteria and archaea using 16S rRNA gene sequences. Nat Rev Microbiol 12:635

Zhang H, Yohe T, Huang L, Entwistle S, Wu P, Yang Z, Busk PK, Xu Y, Yin Y (2018) dbCAN2: a meta server for automated carbohydrate-active enzyme annotation. Nucleic Acids Res 46:W95–W101